JOURNAL OF CHEMICAL INFORMATION AND MODELING

ARTICLE

pubs.acs.org/jcim

Discovery of Novel Selective Serotonin Reuptake Inhibitors through Development of a Protein-Based Pharmacophore

Sankar Manepalli,[†] Laura M. Geffert,[‡] Christopher K. Surratt,[‡] and Jeffry D. Madura*[,†]

[†]Department of Chemistry and Biochemistry and Center for Computational Sciences, Duquesne University, 600 Forbes Avenue, 308 Mellon Hall, Pittsburgh, Pennsylvania 15282, United States

[‡]Division of Pharmaceutical Sciences, Mylan School of Pharmacy, Duquesne University, 600 Forbes Avenue, 411 Mellon Hall, Pittsburgh, Pennsylvania 15282, United States

ABSTRACT: The serotonin transporter (SERT), a member of the neurotransmitter sodium symporter (NSS) family, is responsible for the reuptake of serotonin from the synaptic cleft to maintain neurotransmitter homeostasis. SERT is established as an important target in the treatment of anxiety and depression. Because a high-resolution crystal structure is not available, a computational model of SERT was built based upon the X-ray coordinates of the leucine transporter LeuT, a bacterial NSS homologue. The model was used to develop the first SERT structure-based pharmacophore. Virtual screening (VS) of a small molecule structural library using the generated SERT computational model yielded candidate ligands of diverse scaffolds. Pharmacological analysis of the VS hits identified two SERT-selective compounds, potential lead compounds for further SERT-related medication development.

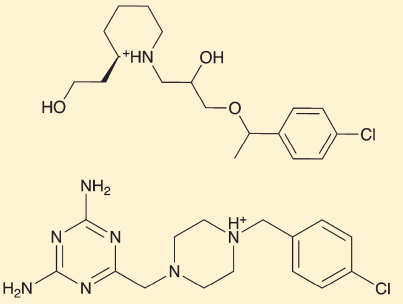

INTRODUCTION

Signaling between cells in the central nervous system is mediated by the controlled release and reuptake of neurotransmitters in the synapse.[1] An excess or deficit of the monoamines serotonin, dopamine, or norepinephrine in the synapse has been associated with various psychiatric and neurological disorders including depression, anxiety, compulsivity, attention deficit hyperactivity disorder (ADHD), substance abuse, Parkinson's disease, and schizophrenia.[2−7] Control of synaptic monoamine levels is affected by the plasma membrane monoamine transporters (MATs), which terminate the action of these biogenic amines via reuptake into the presynaptic cell. The mechanisms of action of drugs related to the above medical conditions typically involve the MAT proteins. Tricyclic antidepressants (TCAs) such as imipramine (Tofranil), developed in the 1950s, alleviate depression by blocking serotonin and norepinephrine transporters (SERT and NET, respectively), thereby extending the lifespan of synaptic serotonin and norepinephrine. Unfortunately, the TCAs also block adrenergic, muscarinic acetylcholine, and histamine receptors, responsible for a plethora of adverse effects.[8,9] Selective serotonin reuptake inhibitors (SSRIs), the next generation of antidepressants led by fluoxetine (Prozac) in the 1980s, carry far fewer adverse effects compared to the TCAs. The SSRIs block SERT, but because the resultant surge of serotonin can activate any of 14 serotonin receptor types, this drug class is not without its own adverse effects.[10−12]

The driving force for MAT uptake of monoamine substrate is electrogenic, harnessing the inward Na^+ gradient across the cell membrane.[13,14] The SERT, NET, and DAT (dopamine transporter) are members of the neurotransmitter:sodium symporter (NSS) family as well as members of a larger group of Na^+ and Cl^- dependent transporters known as the "solute carrier 6" (SLC6) family.[15] The lack of a high-resolution 3-D MAT structure had hindered structure−function and therapeutic development efforts until a breakthrough was achieved in the form of crystallization of the bacterial NSS homologue LeuT, a leucine transporter.[16] The LeuT X-ray structure has provided a template to build credible MAT computational models.[16−21] Although model quality increases with sequence identity with the template, structural similarity also plays a significant role.

In the absence of high-resolution 3D structures for SERT, development of a ligand-based pharmacophore[22−25] or QSAR[26−28] are feasible alternatives to obtain structural information about the binding pocket. Ligand-based approaches analyze a set of ligands and generate possible protein−ligand interaction patterns without knowledge of the protein structure. A limitation of ligand-based approaches is that flexible alignment using dissimilar scaffolds is less reliable; knowledge of the bioactive conformation of at least one active molecule significantly improves alignment accuracy.[29] These limitations can be overcome by using structure-based approaches, in which diverse scaffolds can be used to capture ligand interactions and the binding pocket environment in general. Docking, a structure-based technique, is capable of reliably predicting the bioactive conformation for a cocrystallized ligand.[30] In the absence of an experimental 3D structure, however, a reasonable 3D model can be constructed for a receptor using crystallographic or NMR data from genetically and functionally related proteins.[31,32]

Comparative modeling correctly predicts the 3D fold of a protein in most cases and has often provided insight into the

Received: June 17, 2011
Published: August 12, 2011

ACS Publications © 2011 American Chemical Society

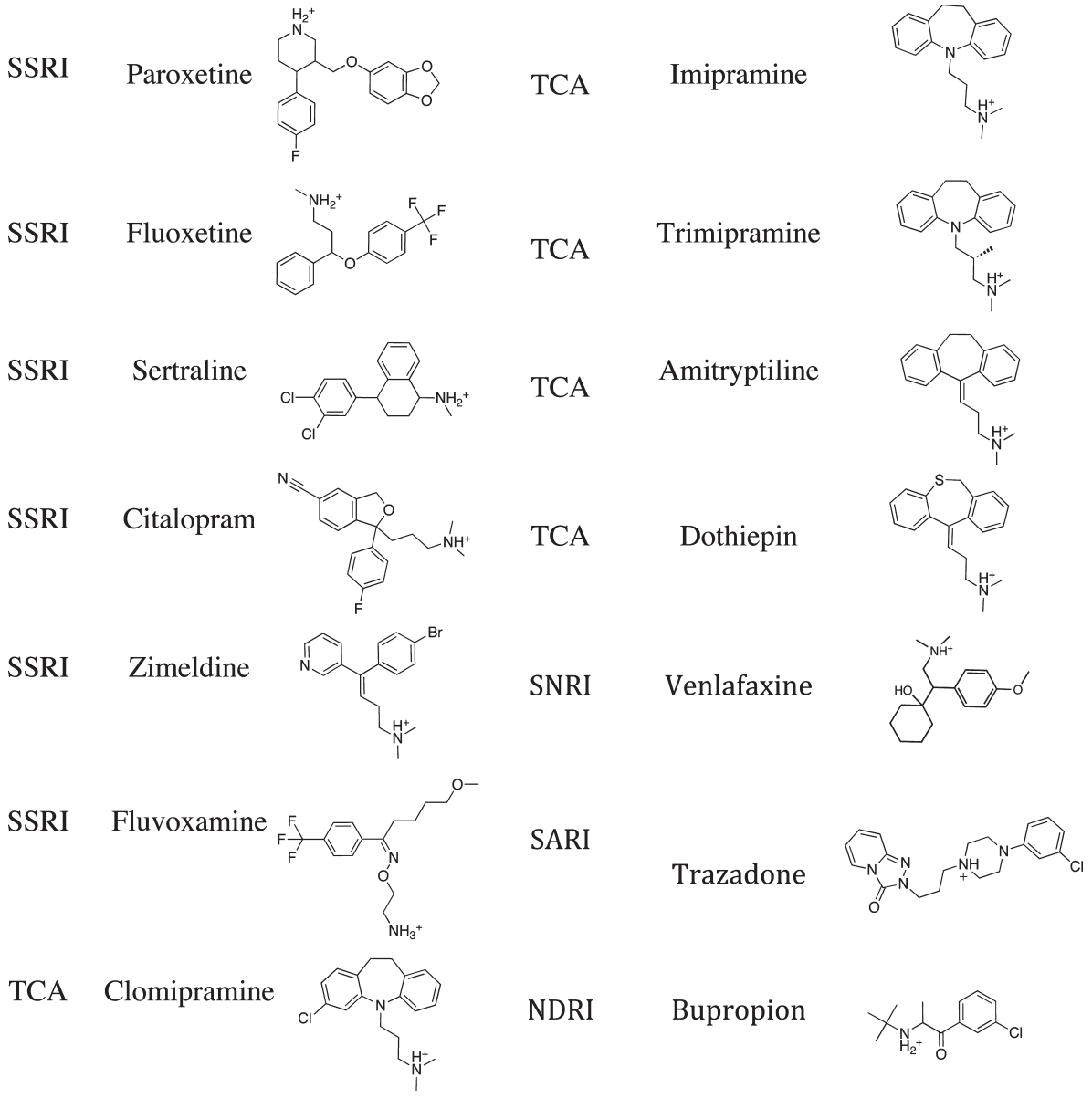

Figure 1. Chemical structures of SERT inhibitors used to develop the pharmacophore.

atomistic details of ligand binding.[33,34] Models created by this method have identified potential binding pockets and have been employed for docking, structure-based pharmacophore generation, and virtual screening (VS) to identify new ligands and their interactions with the protein.[33,35,36] Pharmacophore models, defined as a 3D collection of features essential for bioactivity of a ligand, have been widely employed.[37,38] The approach of combining a pharmacophore with VS has yielded novel structural scaffolds for ligands of a target receptor.[39−44] Application of this technique with the DAT led to the identification of structurally novel VS "hit" compounds which, upon further modification, created a more potent analog through rational drug design.[33,43,45] The present work describes the development of a structure-based pharmacophore and its VS utilization to identify novel ligand structural scaffolds that display SERT selectivity.

RESULTS AND DISCUSSION

Four discrete amino acid sequence alignments with LeuT were generated that primarily differed in the loop regions. Manual refinement of the alignments was conducted to remove gaps within the TM regions. Rotamers of the residue side chains lining the hSERT halogen-binding pocket were selected based on their ability to form a subpocket, as these residues have been reported to be important for binding of certain SSRIs.[21] A total of 80 SERT homology models were built using Discovery Studio (DS) 2.5.1. Five models from each alignment (20 models total) having the lowest discrete optimized protein energy (DOPE) score were chosen for further evaluation. DOPE is an atomistic-based statistical potential for model evaluation and structure prediction. This conformational energy measure reflects the stability of a model relative to other models generated.[46] The models were also deposited into the PDB evaluation server and assessed with

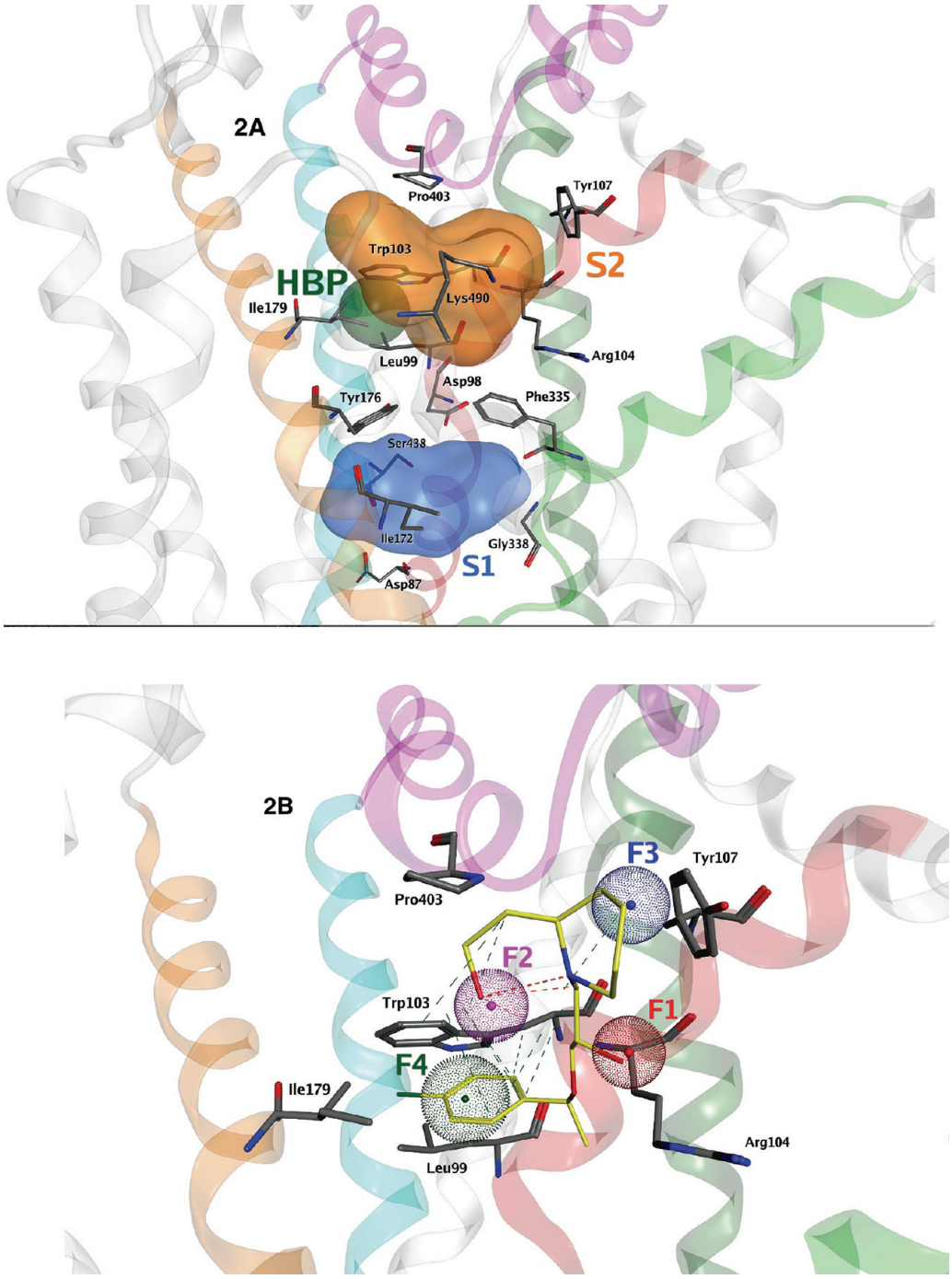

Figure 2. Panel A: Ligand-accessible regions of SERT substrate and inhibitor binding pockets. Regions available to ligands in the S1 (blue), S2 (orange), and HBP (green) pockets are displayed as surfaces. The pocket employed for virtual screening combined the S2 and HBP. Residues defining each pocket are displayed as sticks (atomtype color). For clarity, the TM1 (red), TM3 (orange), TM6 (green), TM8 (cyan), and EL4 (pink) helices are highlighted. Panel B: The pharmacophore employed for VS was comprised of four features (dotted spheres). F1: Donor/acceptor (red). F2: Acceptor (pink). F3: Cation/acceptor (blue). F4: Hydrophobic/π ring (green). Predicted hydrophobic (green dashed lines) and H-bonding (red dashed lines) are shown for the VS hit compound SM-10 (yellow sticks with heteroatoms in green (halogen), red (oxygen), or blue (nitrogen)).

respect to stereochemical quality.[47] The plots generated by the server were evaluated for unusual phi-psi angles, bond lengths, bond angles, and van der Waals contacts. Two models were selected for further evaluation, specifically their fitness in a 3D environment assessed by Profiles-3D. This DS module assesses the protein's tertiary structure compatibility with its sequence. Finally, spatial overlap of the model and template polypeptide backbone atoms was examined to check the integrity of the model's TM domains and the volume of its binding pocket. On this basis, "Model 1" was chosen for further studies.

The MOE alpha site finder was used to identify possible ligand sites in Model 1. A site exposed to the extracellular space was chosen based on evidence for inhibitors binding in this vestibule.[21] A sphere with a radius of 8 Å was created to constrain the resulting

dx.doi.org/10.1021/ci200280m |J. Chem. Inf. Model. 2011, 51, 2417–2426

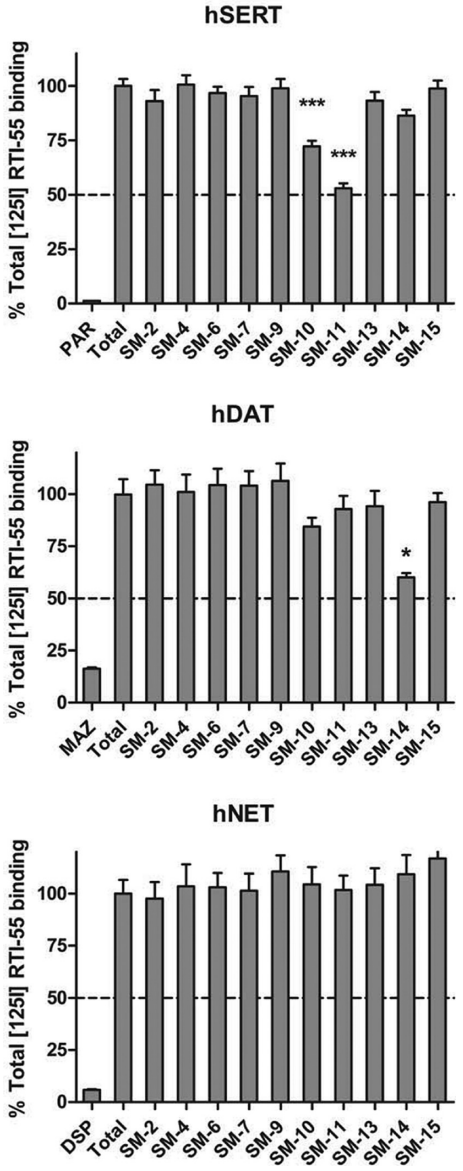

Figure 3. VS hit compound in vitro MAT binding screen. Compounds at 10 μM final concentration were tested for the ability to inhibit [^{125}I]-RTI-55 binding at hSERT HEK293 cells (top panel), hDAT N2A neuroblastoma cells (middle panel), or hNET HEK293 cells (bottom panel). Nonspecific binding was assessed by the presence of 10 μM paroxetine (PAR), mazindol (MAZ), or desipramine (DSP) for SERT, DAT, and NET, respectively. Data represent n = 3 independent experiments performed in duplicate. Data are presented as the mean ± sem and were analyzed by one-way ANOVA with Dunnett's multiple comparison posthoc test. *P < 0.05 vs total binding for that assay. ***P < 0.0001 vs total binding for that assay.

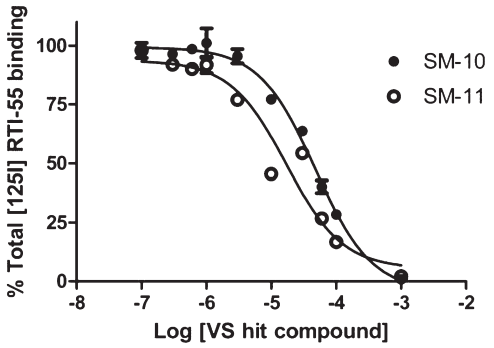

Figure 4. Saturation binding of VS hit compounds SM-10 (closed circles) and SM-11 (open circles) at hSERT HEK293 cells. Binding affinity K_i values were determined via displacement of [^{125}I]-RTI-55. n = 3 experiments.

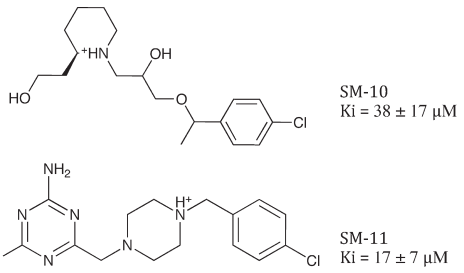

Figure 5. Structures and hSERT binding affinities of SM-10 and SM-11.

docked poses, in keeping with recent reports.[18,21] The combination of proxy triangle as the placement method and force field refinement with an affinity scoring function yielded MOE docking poses of leucine into LeuT with an rmsd of 0.31 Å (data not shown). This strategy was next used to dock each of 16 structurally diverse antidepressants (Figure 1), possessing a large range of SERT binding affinities (0.1 nM−9100 nM). It is acknowledged that certain SSRI ligands used in the docking have been reported to access the interior S1 substrate pocket;[48] however, the VS pocket employed in this study contained elements of the vestibular (S2 substrate) pocket and the halogen binding pocket (HBP) (Figure 2A). The latter pocket is defined in part by hSERT residues Leu-99 (TM 1), Trp-103 (TM 1), and Ile-179 (TM 3). The ligand-accessible region of the HBP (green cloud) is adjacent to that of the S2 pocket (orange cloud) (Figure 2A); the HBP appears to be important for recognition of halogen-containing inhibitors. Poses in which the halogen atom of the ligand was directed toward this pocket were thus favored. A consensus was developed by overlaying the highest-ranked poses to generate a "common interaction pattern".

Residues identified as common interaction points were then chosen to develop a 3D pharmacophore (Figure 2B). Pharmacophore feature F1 of radius 1 Å was created midway between Arg-104 (TM 1) and Glu-493 (TM 10) to capture possible ionic or H-bond interactions, particularly with protonated ligand nitrogen atoms. Previous reports of SERT-based pharmacophore models indicated the importance of a positively charged nitrogen atom.[49,50] Feature F2 (radius 1 Å) was created in the vicinity of Lys-490 (TM 10) to capture possible H-bond interactions. The lysine side chain is among the more flexible of the naturally occurring amino acids; 78 rotamers were possible for Lys-490. The rotamer oriented toward the vestibular pocket, analogous to Asp-401 in LeuT, was chosen to capture possible interactions with ligands. Asp-401 is reported to interact with different antidepressants in LeuT crystal structures;[21] thus, Lys-490 would be expected to play a similar role in hSERT. Feature F3 (radius 1 Å) was created to capture H-bond or cation-π interactions with Tyr-107 (TM 1). Residues 104−106 of hSERT TM 1b are analogous to LeuT residues 30−32, although hSERT Tyr-107 and LeuT Val-33 differ substantially regarding the nature of potential ligand

interactions. Feature F4 (radius 1.5 Å) in the HBP was designed for hydrophobic interactions believed to be important in recognizing SSRIs. Residues lining the pocket are conserved between hSERT and LeuT.[21] Substitution of the hSERT TM 3 residue Ile-179 (Ile-111 in LeuT) with alanine, phenylalanine, or aspartic acid increased SSRI substrate uptake inhibition potency by 7−1080-fold.[21]

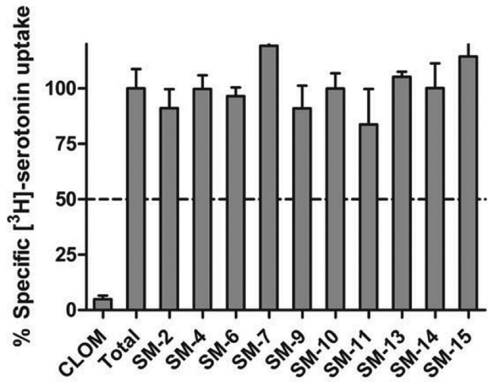

Figure 6. VS hit compound in vitro serotonin uptake inhibition screen. Compounds at 10 μM final concentration were tested for the ability to inhibit [^{3}H]-serotonin uptake by hSERT HEK293 cells. Nonspecific radioligand uptake was assessed by the presence of 10 μM clomipramine (CLOM). Data represent n = 3 independent experiments performed in duplicate. Data are presented as the mean ± sem and were analyzed by one-way ANOVA with Dunnett's multiple comparison posthoc test. *P < 0.05 vs total uptake for that assay. **P < 0.001 vs total uptake for that assay.

The TM 1 mutations Ala77Gly in hNET and Ala81Gly in hDAT were observed to improve SSRI affinity, suggesting a negative influence of the methyl side chain of alanine on SSRI binding. Finally, an exclusion volume was added to make the pharmacophore more stringent and selective.

Approximately one million members of the ZINC small molecule structural library database[51] were screened with the hSERT pharmacophore for possible "hit" compounds (those predicted to be SERT ligands). A total of 4097 molecules were acceptable to the pharmacophore filter. Docking of this subset into the SERT model followed by monitoring of affinity dG scores with visual inspection of the resulting poses yielded 68 preferred compounds. Due to lack of availability, only ten of the top 15 compounds (labeled SM-1 to SM-15) were initially tested for hSERT, hDAT, or hNET affinity in single point in vitro binding assays. Two compounds, SM-10 and SM-11, at 10 μM significantly displaced the cocaine analog [^{125}I]-RTI-55 from hSERT membranes, indicating measurable hSERT affinity. At the same final concentration, these two compounds did not displace the radioligand at hDAT or hNET cells. SM-14, curiously, displaced [^{125}I]-RTI-55 at hDAT cells alone (Figure 3). A DAT binding affinity K_i value of 15.6 ± 2.4 μM (mean ± s.e.m.) and a dopamine uptake inhibition potency IC_{50} value of 10.5 ± 4.6 μM were observed (manuscript in preparation). SM-10 and SM-11 were further characterized at hSERT HEK293 membranes in competition assays to obtain K_i values for inhibition of [^{125}I]-RTI-55 binding. hSERT K_i values of 38 ± 17 μM and 17 ± 7 μM were obtained for SM-10 and SM-11, respectively (Figure 4). SM-10 and SM-11 were also screened for the ability to inhibit uptake of [^{3}H]-serotonin by intact hSERT HEK293 cells.

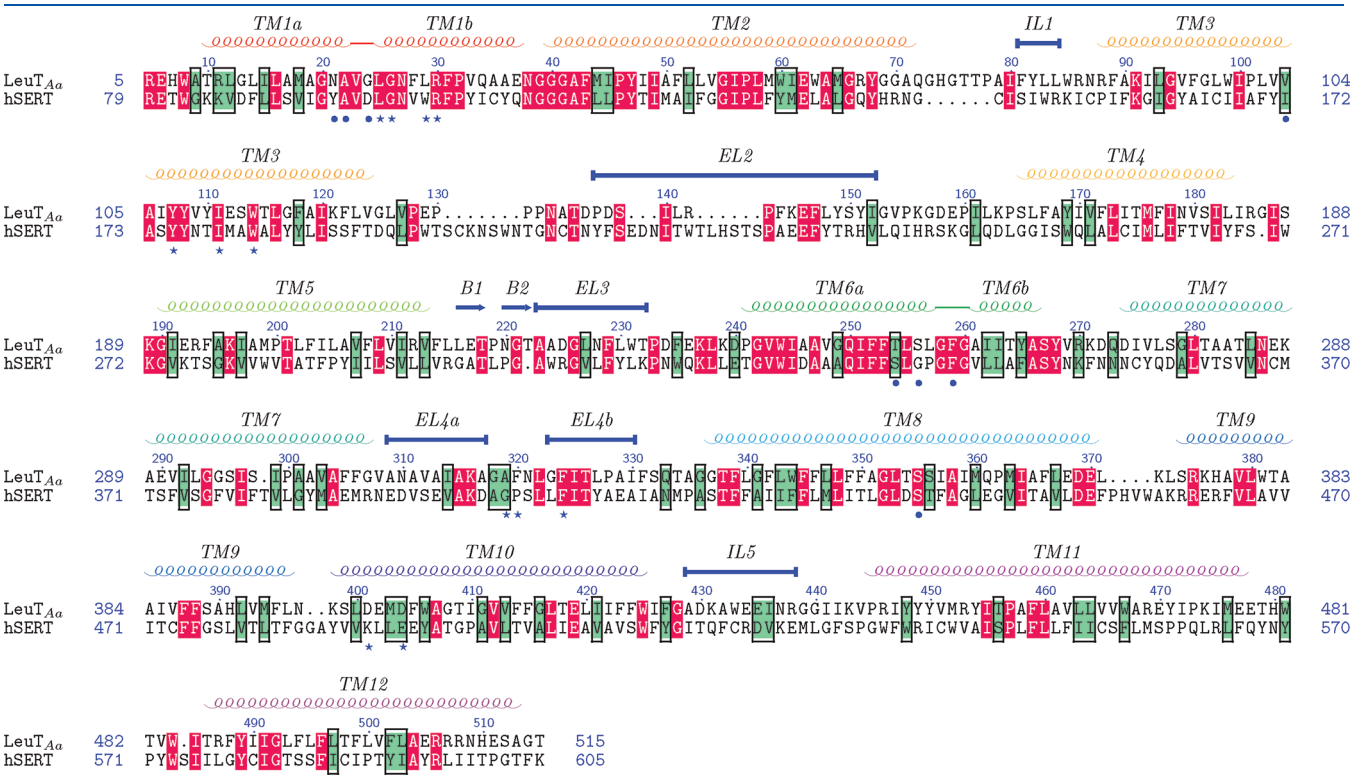

Figure 7. Alignment of LeuT$_{Aa}$ and hSERT amino acid sequences used to build Model 1. Identical (red) and similar (green) aligned residues are indicated. The dots and stars correspond to residues lining S1 and S2 pockets, respectively. Transmembrane and connecting loop topology is displayed above the sequences. Gaps relative to the other sequence are represented by dots. Position of the residue in its respective chain is indicated before and after each line of sequence. The figure was prepared using TEXshade.[79]

dx.doi.org/10.1021/ci200280m |J. Chem. Inf. Model. 2011, 51, 2417–2426

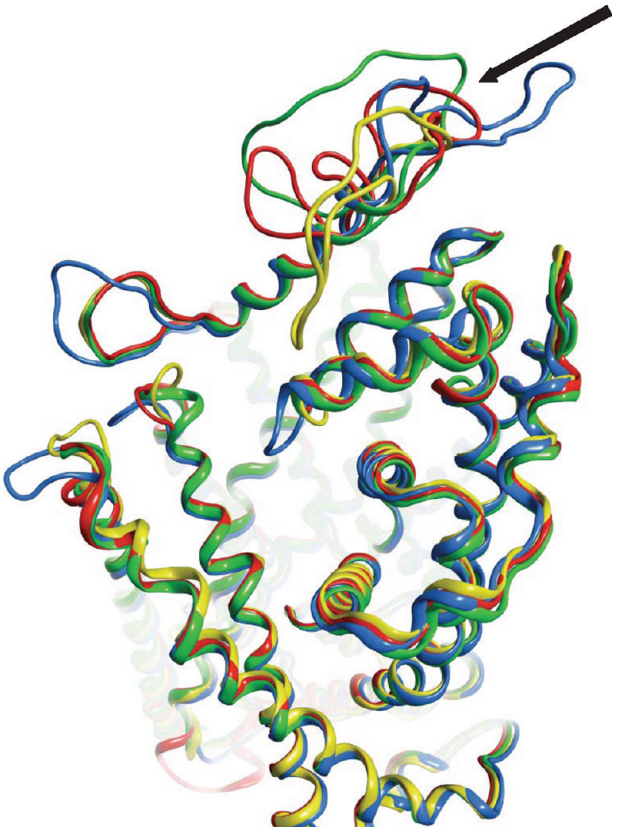

Figure 8. Polypeptide backbone superposition of the four homology SERT models. Good overall spatial overlap was observed for Models 1 (Manepalli et al.; red), 2 (Beuming et al.;[67] blue), 3 (Yamashita et al.;[16] yellow) and 4 (Celik et al.;[66] green), with essentially perfect overlap of TM domains. EL2 (arrow) was the most divergent region among the four models.

Because no inhibition of [^{3}H]-serotonin uptake was detected at the 10 μM final concentration employed for these two VS hit compounds (Figure 5), IC_{50} values were not obtained. Given their structural flexibility (Figure 6), SM-10 and SM-11 greatly differ from the SSRIs and TCAs that were employed to develop the pharmacophore.

Given the high sequence similarity (~50%, as calculated with BLAST) among the three hMATs, finding a specific inhibitor that targets a single transporter is a challenging task. VS is more precarious with the additional inhibitor binding pocket uncertainty associated with a homology model built using a template sharing <30% sequence identity (Figure 7). Because of this handicap, and because the goal of the study was to identify SERT ligands of novel structural scaffold, a very high concentration of VS hit compound relative to the SERT ligand radiotracer (100,000-fold) was employed in the pharmacologic screen. The observation that most of the VS hits showed no ability to displace the radioligand at the SERT-HEK cells confirms that the huge molar ratio of VS compound:radiotracer was itself insufficient for decreasing radiotracer binding (i.e., some SERT affinity is required to register a response in this assay).

The two VS hits pharmacologically verified as SERT ligands displayed micromolar K_i values. These binding affinities are very low compared to the nanomolar or better SERT affinities of certain SSRI therapeutics. Inhibition of serotonin uptake was not observed for any VS hit compound at the 10 μM screening concentration. Substrate uptake inhibition potency is often lower than binding affinity for a given MAT inhibitor, possibly due to differences in MAT conformational or population requirements for the two processes.[52,53] The 10 μM SM-10 or SM-11 concentration employed may be above the threshold for detecting SERT ligand binding but below the threshold for detecting serotonin uptake inhibition.

Micromolar affinities for VS hit compounds are common when homology models are employed.[54−61] From this research team, the first reported VS effort based on a DAT homology model yielded a hit compound (MI-4) with low micromolar DAT affinity and slightly better (high nanomolar) SERT affinity. Without modification, this compound displayed antipsychostimulant and antidepressant properties (ref 43 and unpublished data). The same VS effort using a DAT model yielded a hit compound (MI-17) with a SERT K_i value of 284 nM. An MI-17 analog designed to increase SERT selectivity resulted in a compound with a SERT K_i value of 37 nM and SERT:DAT and SERT:NET selectivity ratios of 50 and over 200, respectively.[45] Thus, VS hit compounds with micromolar affinities appear to be useful as lead compounds for medication development.

CONCLUSION

To our knowledge this is the first study to identify novel SERT-selective reuptake inhibitors through VS performed with a hSERT homology model. Conventional drug development usually involves creation of analogs of established ligands for a given receptor. In contrast, the VS approach affords the possibility of discovering ligands with very different scaffolds, ligands that in all likelihood would never be otherwise identified for that receptor. In the case of the SERT, inhibitors of novel scaffold provide new opportunities for development of rationally designed multisite drugs (e.g., SERT/5-HT_{2A}/5-HT_3 blockers) that address the therapeutic goal while mitigating the adverse effects associated with the SSRI drug class. It is anticipated that the two SM compounds described herein should serve as lead compounds toward the treatment of depression, anxiety, and other serotonin-related disorders.

METHODS

Materials. [^{125}I]-RTI-55 and [^{3}H]-serotonin were purchased from PerkinElmer (Foster City, CA). VS hit compounds were purchased from Enamine and Molport. The N2A-hDAT cell line was a gift from Dr. Margaret Gnegy (University of Michigan). HEK293 cells stably transfected with hSERT or hNET were prepared in collaboration with Dr. Mads Larsen and Dr. Susan Amara (University of Pittsburgh, Pittsburgh, PA).

Construction of SERT Homology Models. *Polypeptide Sequence Retrieval and Alignment.* The FASTA sequence for human SERT was downloaded from the Uniprot database (accession number P31645).[62] The X-ray crystal structure of the *Aquifex aeolicus* protein LeuT (2a65) was used as a template and downloaded from the Protein Data Bank (PDB).[63] The template was checked for missing residues using the "protein reports and utilities" module in Discovery Studio (DS) 2.5.1.[64] Prior to modeling efforts, the missing residues Asn-133 and Ala-134 of the second extracellular loop (EL2) were built into the LeuT template and subjected to the DS loop refinement protocol. Different hSERT models were created using the Align2d methodology[65] and the three previously proposed sequence alignments.[16,66,67]

hSERT Model 1: Manepalli et al. Alignment (This Article). The sequences of hSERT and modified LeuT were aligned using the "align sequence to templates" protocol in DS. An alignment similar to Celik et al.[66] was generated, with minor manual modifications further increasing the sequence identity with LeuT (Figure 7). N- and C-terminal overhangs were deleted, increasing sequence identity to 24% and sequence similarity to 47%. The hSERT model sequence began at Arg-79 in the N-terminal tail and ended with Lys-605 in the C-terminal tail. The "build homology model" protocol in DS, which employs MODELLER version 9v4,[31] was used to construct 20 hSERT models. The models were further refined (see "Model validation") and ranked by discrete optimized protein energy[46] (DOPE) score. The model with the best DOPE score was designated "Model 1".

hSERT Model 2: Beuming et al. Alignment. The hSERT query sequence and modified LeuT were loaded into DS and aligned as described by Beuming et al.[67] Terminal residues not having the matching template coordinates at both ends were omitted, and 20 models were built and assigned DOPE scores as described above. Models based on this alignment resulted in EL2 positioned directly above the substrate permeation pore, which would likely have influenced ligand docking. The dangling EL2 was adjusted using the DS loop refinement protocol. Models were then evaluated using the "verify protein" protocol, which assesses the score of each residue in the known 3D environment. This was followed by superposition of the hSERT model onto LeuT to check for TM domain coincidence. The final version was designated "Model 2".

hSERT Model 3: Yamashita et al. Alignment. The hSERT query sequence and modified template were aligned as proposed by Yamashita et al.[16] N- and C-terminal overhangs were deleted, leaving 527 hSERT residues. The optimal model resulting from this alignment was designated as "Model 3".

hSERT Model 4: Celik et al. Alignment. Twenty hSERT models were built with DS as described above but following the proposed Celik et al. alignment,[66] which offered a sequence identity match comparable to the Manepalli alignment and greater than the Beuming and Yamashita alignments. A 527-residue hSERT polypeptide was used to develop "Model 4", as described for Model 1.

Model Refinement and Validation. Five models from each of the four alignment groups were chosen based on DOPE scores. The stereochemical quality of the preferred models was assessed with the validation server used to evaluate structures deposited into PDB.[46] From each group of five, two models were then chosen based on their having the fewest outliers on the phi-psi angle Ramachandran plot. These two models were evaluated for 3D fold, using the "verify protein" protocol in DS. This protocol reduces 3D structures to a simplified 1D representation, compares this to the 1D amino acid sequence, and assigns a score. This score is compared to the expected high and low scores for the sequence predicted from statistical analysis of high-resolution PDB structures.

TM domain assembly and ligand binding pocket volume were checked by superposing the SERT models onto the LeuT model using MOE (Figure 8).[68] A single hSERT model was selected for each of the four groups. The all-atom force field Assisted Model Building with Energy Refinement (AMBER99)[69,70] was used to add hydrogen atoms and partial charges to the models. Keeping the non-hydrogen atoms fixed in space, hydrogen atoms were minimized with a convergence criterion of 0.05 kcal/mol. The final hSERT models chosen from each alignment were further optimized to minimize the outliers and avoid unnecessary protein contacts. Of the four models, Model 1 had the smallest rmsd on superposition with LeuT and maximal ligand binding pocket volume, similar to LeuT.

Ligand Binding Site Delineation and Docking; Pharmacophore Development. The alpha site finder function of MOE 2008.09 was used to identify possible ligand binding sites in Model 1. The site finder is purely geometric; no energy terms are used. Alpha spheres within the hSERT model that were too exposed to solvent were eliminated; spheres that corresponded to locations of tight atomic packing in the model were retained. Spheres were classified as either "hydrophobic" or "hydrophilic" depending on the potential for hydrogen bonding. Following the default settings, alpha spheres were clustered to produce a collection of putative binding sites that are ranked according to the number of hydrophobic atoms within contact distance of the spheres. Finally, dummy atoms were created in the S1 and S2 pockets to specify the algorithm to dock the ligands.

Ligand coordinates were obtained from the small molecule crystal database CCSD (Cambridge Crystallographic Structural Database).[71,72] Ligands having no coordinates were drawn using MOE. Partial charges and hydrogen atoms were added to all ligands using Merck Molecular Force Field 94x (MMFF-94x).[73−75] Ligand geometry was optimized via energy minimization with a conjugated gradient truncated Newton optimization algorithm with convergence criteria = 0.01 kcal/mol, $\varepsilon = 1$. Leucine or selected TCA drugs were first docked with the LeuT model to test for consistency with the reported cocrystal structures.[16,21] Atom placement methods including proxy triangle, alpha triangle, and triangle matcher were employed, as were refinement techniques using grid-based and force field-based methods. The combination that produced poses very close to the crystal structure (<1 Å) was chosen for hSERT docking. Interaction plots for all docked poses of different antidepressants in hSERT were generated using the MOE ligand interaction module.[76] A consensus of residues and their predicted ligand interactions was developed and used in creating the pharmacophore features for the vestibular ligand-binding pocket.

A pharmacophore feature was generated at each amino acid side chain−ligand interaction point obtained from initial docking iterations. Pharmacophore points F1, F2, F3 (each with a radius of 1 Å) and F4 (radius = 1.5 Å) were delineated to better encompass the hydrophobic features of the docked ligands. An excluded volume was created, and the algorithm was assigned a penalty to poses that encroached on this space. The final pharmacophore product was tested using a database containing known hSERT ligands and decoy ligands. The pharmacophore model successfully discriminated the classic hSERT ligands from the decoys.

Virtual Screening. An 18 million entry "all-purchasable" subset of the ZINC database was downloaded.[51] The subset was "washed" by importing the collection into MOE, which removes unwanted salts, ions, and disconnected molecular fragments from the database. The Lipinski's Rule of Five descriptor was applied to the database to remove nondrug-like molecules.[77] Compounds with reactive groups were removed by further screening the database using a toxic moiety descriptor. From this database a subset containing approximately one million compounds was selected for further use. Tautomers and protomers of these entries were generated at physiological pH. Using the "import conformation" module of MOE, different conformations were generated and minimized using the MMFF94x force field; conformations with strain energy 4 kcal/mol or more above the lowest energy conformation were discarded. This final database

was screened using the 4-point pharmacophore. "Hit" compounds acceptable to the pharmacophore filter were further screened to ensure the presence of halogens and a molecular weight <350 Da, features common to most of the known antidepressants. These steps yielded a pool of 4097 hit compounds. Three hSERT docking iterations were performed with this pool of structures. Affinity scores < −6.0 kcal/mol plus visual inspection were used to condense the pool to 68 candidate ligands. Of these, 10 of the top-ranked 15 compounds (coded "SM-1" through "SM-15") were procured from various sources and pharmacologically tested.

Pharmacology. *In Vitro VS Compound Binding Screen.* Compounds identified from the virtual screen were purchased and dissolved in 100% DMSO to a concentration of 10 mM. Initial one-point competition binding assays were conducted using 10 μM final concentration of VS hit compound and 0.1 nM of the radiolabeled cocaine analog [^{125}I]-RTI-55, a radioligand with high affinity at all three MATs. Stably transfected HEK293-hSERT membranes or N2A-hDAT or HEK293-hNET whole cells were employed for all binding assays. Nonspecific binding was determined by inclusion of 10 μM paroxetine, mazindol, or desipramine for hSERT, hDAT, or hNET assays, respectively. Screening results were analyzed with one-way ANOVA ($P < 0.05$) with a posthoc Dunnett's Multiple Comparison Test.

hSERT Membrane Binding Assay. hSERT binding affinities were obtained by displacement of [^{125}I]-RTI-55 in membrane binding assays. Membrane was prepared from stable hSERT-HEK cells grown at 37 °C in a 5% CO_2 environment on 150 × 25 mm plates. At 95% confluence (3 days of growth), cells were washed twice with 10 mL of cold phosphate-buffered saline (DPBS). An additional 10 mL of DPBS was added, and cells were harvested by scraping and transferred to cold centrifuge tubes (15 mL), followed by centrifuging for 10 min at low speed (700 × g). After removal of the supernatant, the cell pellet was resuspended in 500 uL of cold TE buffer (50 mM Tris, 1 mM EDTA, pH 7.5). Following centrifuging for 30 min at 100,000*g* at 4 °C, the supernatant was discarded, and the pellet was frozen for later use or resuspended in ice-cold binding buffer (50 mM Tris, pH 7.5, 100 mM NaCl). Each sample was analyzed for protein content using the Bradford protein assay. For competition binding, membrane was incubated with [^{125}I]-RTI-55 (0.1 nM concentration) and increasing concentrations of cold competitor (1 nM to 1 mM) or 10 μM paroxetine to measure nonspecific binding. Reactions were carried out in 12 × 75 mm borosilicate glass tubes with gentle shaking at room temperature for 1 h and terminated by rapid filtration through GF/B filters (Schleicher and Schuell, Keene, NH) presoaked in 0.5% polyethylenimine solution (v/v). Filters were washed twice with 5 mL of cold 50 mM Tris buffer and transferred to vials. Radioactivity was determined using a Beckman gamma counter. For saturation binding assays, data were analyzed with GraphPad Prism 5.0 software. IC_{50} values were generated and converted to K_i values using the Cheng-Prusoff equation ($K_i = IC_{50}/(1+([\text{RTI-55}]/K_d\ \text{RTI-55}))$).[78]

hDAT and hNET Whole Cell Binding Assays. Whole-cell competition binding assays were performed for hDAT and hNET using stable hDAT-N2A or hNET-HEK293 cell lines, respectively, grown at 37 °C in a 5% CO_2 environment. Cell monolayers were grown in 24-well plates to >90% confluence. Cells were washed twice with 1 mL of KRH buffer (25 mM HEPES, pH 7.3, 125 mM NaCl, 4.8 mM KCl, 1.3 mM $CaCl_2$, 1.2 mM $MgSO_4$, 1.2 mM KH_2PO_4, 5.6 mM glucose) supplemented with 50 mM ascorbic acid (KRH/AA). Cells were incubated for 15 min with 1 nM [^{125}I]-RTI-55 supplemented with tropolone (total volume of 500 μL) along with increasing concentrations of drug or 10 μM mazindol (hDAT) or 10 μM desipramine (hNET). Following incubation, cells were washed twice with 1 mL of KRH/AA buffer and then treated with 1 mL of 1% SDS with gentle shaking at room temperature for 1 h. Cell lysates were transferred into vials. Radioactivity was determined using a Beckman gamma counter and analyzed using GraphPad Prism 5.0 as described above.

Serotonin Uptake Inhibition Screen. One-point competition binding assays were performed using stably transfected HEK293-hSERT whole cells grown to >90% confluence on 24-well plates. Cells were washed with KRH buffer and then preincubated with 10 μM VS hit compound for 10 min, followed by addition of 10 nM [^{3}H]-serotonin. After an additional 5 min, cells were washed twice and then treated with 1% SDS and shaken for 1 h. Lysates were transferred to 5 mL of scintillation fluid, and radioactivity was detected using a Beckman liquid scintillation counter. Nonspecific radioligand uptake was determined in the presence of 10 μM clomipramine.

AUTHOR INFORMATION

Corresponding Author
*E-mail: madura@duq.edu.

ACKNOWLEDGMENT

We thank Dr. Tammy Nolan for creating the hSERT and hNET HEK cell lines and for helpful discussions in the development of the manuscript and thank Drs. Mads Larsen and Susan Amara for collaboration in creating the hSERT and hNET cell lines. This work was supported by NIDA grants DA026350 (to C.K.S) and NIH grant DA027806, Department of Education equipment grants P116Z050331 and P116Z080180 (to J.D.M).

ABBREVIATIONS

MAT, monoamine transporter protein; hSERT, plasma membrane human serotonin transporter protein; hDAT, plasma membrane human dopamine transporter protein; hNET, plasma membrane human norepinephrine transporter protein; SSRI, selective serotonin reuptake inhibitor; VS, virtual screening; DOPE, discrete optimized protein energy

REFERENCES

(1) Amara, S. G.; Kuhar, M. J. Neurotransmitter Transporters: Recent Progress. *Annu. Rev. Neurosci.* **1993**, *16*, 73–93.

(2) Hahn, M. K.; Blakely, R. D. Monoamine Transporter Gene Structure And Polymorphisms In Relation To Psychiatric And Other Complex Disorders. *Pharmacogenomics J.* **2002**, *2* (4), 217–235.

(3) Heinz, A.; Mann, K.; Weinberger, D. R.; Goldman, D. Serotonergic dysfunction, negative mood states, and response to alcohol. *Alcohol.: Clin. Exp. Res.* **2001**, *25* (4), 487–495.

(4) Klimek, V.; Stockmeier, C.; Overholser, J.; Meltzer, H. Y.; Kalka, S.; Dilley, G.; Ordway, G. A. Reduced levels of norepinephrine transporters in the locus coeruleus in major depression. *J. Neurosci.* **1997**, *17* (21), 8451–8458.

(5) Robertson, D.; Flattem, N.; Tellioglu, T.; Carson, R.; Garland, E.; Shannon, J. R.; Jordan, J.; Jacob, G.; Blakely, R. D.; Biaggioni, I. Familial orthostatic tachycardia due to norepinephrine transporter deficiency. *Ann. N.Y. Acad. Sci.* **2001**, *940*, (Neuro-Cardiovascular Regulation), 527-543.

(6) Miller, G. M.; De La Garza, R., II; Novak, M. A.; Madras, B. K. Single nucleotide polymorphisms distinguish multiple dopamine transporter alleles in primates: Implications for association with attention deficit hyperactivity disorder and other neuropsychiatric disorders. *Mol. Psychiatry* **2001**, *6* (1), 50–58.

(7) Ozaki, N.; Goldman, D.; Kaye, W. H.; Plotnicov, K.; Greenberg, B. D.; Lappalainen, J.; Rudnick, G.; Murphy, D. L. Serotonin transporter missense mutation associated with a complex neuropsychiatric phenotype. *Mol. Psychiatry* **2003**, *8* (11), 933–936.

(8) Cusack, B.; Nelson, A.; Richelson, E. Binding of antidepressants to human brain receptors: Focus on newer generation compounds. *Psychopharmacology* **1994**, *114* (4), 559–565.

(9) Green, J. P.; Maayani, S. Tricyclic antidepressant drugs block histamine H2 receptor in brain. *Nature* **1977**, *269* (5624), 163–165.

(10) Ferguson, J. M. SSRI antidepressant medications: Adverse effects and tolerability. *Prim. Care Companion J. Clin. Psychiatry* **2001**, *3* (1), 22–27.

(11) Frazer, A. Pharmacology of antidepressants. *J. Clin. Psychopharmacol.* **1997**, *17* (Suppl 1), 2S–18S.

(12) Goldberg, R. J. Selective serotonin reuptake inhibitors: Infrequent medical adverse effects. *Arch. Fam. Med.* **1998**, *7* (1), 78–84.

(13) Rudnick, G. Mechanisms of biogenic amine neurotransmitter transporters. In *Neurotransmitter transporters: structure, function, and regulation;* 1997; pp , 73−100.

(14) Masson, J.; Sagne, C.; Hamon, M.; El Mestikawy, S. Neurotransmitter transporters in the central nervous system. *Pharmacol. Rev.* **1999**, *51* (3), 439–464.

(15) Nelson, N. The family of Na+/Cl- neurotransmitter transporters. *J. Neurochem.* **1998**, *71* (5), 1785–1803.

(16) Yamashita, A.; Singh, S. K.; Kawate, T.; Jin, Y.; Gouaux, E. Crystal structure of a bacterial homologue of Na+/Cl--dependent neurotransmitter transporters. *Nature* **2005**, *437* (7056), 215–223.

(17) Zhou, Z.; Zhen, J.; Karpowich, N. K.; Goetz, R. M.; Law, C. J.; Reith, M. E. A.; Wang, D.-N. LeuT-Desipramine structure reveals how antidepressants block neurotransmitter reuptake. *Science* **2007**, *317* (5843), 1390–1393.

(18) Singh, S. K.; Yamashita, A.; Gouaux, E. Antidepressant binding site in a bacterial homologue of neurotransmitter transporters. *Nature* **2007**, *448* (7156), 952–956.

(19) Singh, S. K.; Piscitelli, C. L.; Yamashita, A.; Gouaux, E. A competitive inhibitor traps leuT in an open-to-out conformation. *Science* **2008**, *322* (5908), 1655–1661.

(20) Quick, M.; Lund Winther, A.-M.; Shi, L.; Nissen, P.; Weinstein, H.; Javitch, J. A. Binding of an octylglucoside detergent molecule in the second substrate (S2) site of LeuT establishes an inhibitor-bound Conformation. *Proc. Natl. Acad. Sci.* **2009**, *106* (14), 5563–5568.

(21) Zhou, Z.; Zhen, J.; Karpowich, N. K.; Law, C. J.; Reith, M. E.; Wang, D. N. Antidepressant specificity of serotonin transporter suggested by three LeuT-SSRI structures. *Nat. Struct. Mol. Biol.* **2009**, *16* (6), 652–657.

(22) Orus, L.; Perez-Silanes, S.; Oficialdegui, A.-M.; Martinez-Esparza, J.; Del Castillo, J.-C.; Mourelle, M.; Langer, T.; Guccione, S.; Donzella, G.; Krovat, E. M.; Poptodorov, K.; Lasheras, B.; Ballaz, S.; Hervias, I.; Tordera, R.; Del Rio, J.; Monge, A. Synthesis and molecular modeling of new 1-Aryl-3-[4-arylpiperazin-1-yl]-1-propane derivatives with high affinity at the serotonin transporter and at 5-HT1A Receptors. *J. Med. Chem.* **2002**, *45* (19), 4128–4139.

(23) Zhang, S.; Fernandez, F.; Hazeldine, S.; Deschamps, J.; Zhen, J.; Reith, M. E. A.; Dutta, A. K. Further structural exploration of trisubstituted asymmetric pyran derivatives (2S,4R,5R)-2-Benzhydryl-5-benzylamino-tetrahydropyran-4-ol and their corresponding disubstituted (3S,6S) pyran derivatives: A proposed pharmacophore model for high-Affinity interaction with the dopamine, serotonin, and norepinephrine transporters. *J. Med. Chem.* **2006**, *49* (14), 4239–4247.

(24) Chang, C.; Ekins, S.; Bahadduri, P.; Swaan, P. W. Pharmacophore-Based discovery of ligands for drug transporters. *Adv. Drug Delivery Rev.* **2006**, *58* (12−13), 1431–1450.

(25) MacDougall, I. J. A.; Griffith, R. Pharmacophore design and database searching for selective monoamine neurotransmitter transporter ligands. *J. Mol. Graphics Modell.* **2008**, *26* (7), 1113–1124.

(26) Wellsow, J.; Machulla, H.-J.; Kovar, K.-A. 3D QSAR Of serotonin transporter ligands: CoMFA And CoMSIA studies. *Quant. Struct.-Act. Relat.* **2002**, *21* (6), 577–589.

(27) Pratuangdejkul, J.; Schneider, B.; Jaudon, P.; Rosilio, V.; Baudoin, E.; Loric, S.; Conti, M.; Launay, J. M.; Manivet, P. Definition of an uptake pharmacophore of the serotonin transporter through 3D-QSAR analysis. *Curr. Med. Chem.* **2005**, *12* (20), 2393–2410.

(28) Kharkar, P. S.; Reith, M. E. A.; Dutta, A. K. Three-dimensional Quantitative structure-activity relationship (3D QSAR) and pharmacophore elucidation of tetrahydropyran derivatives as serotonin and norepinephrine transporter inhibitors. *J. Comput.-Aided Mol. Des.* **2008**, *22* (1), 1–17.

(29) *Virtual Screening for Bioactive Molecules*; Boehm, H.-J., Schneider, G., Eds.; 2000; pp 307−308.

(30) B-Rao, C.; Subramanian, J.; Sharma, S. D. Managing protein flexibility in docking and Its applications. *Drug Discovery Today* **2009**, *14* (7/8), 394–400.

(31) Sali, A.; Blundell, T. L. Comparative protein modelling by satisfaction of spatial restraints. *J. Mol. Biol.* **1993**, *234* (3), 779–815.

(32) Chothia, C.; Lesk, A. M. The relation between the divergence of sequence and structure in proteins. *EMBO J.* **1986**, *5* (4), 823–826.

(33) Indarte, M.; Madura, J. D.; Surratt, C. K. Dopamine transporter comparative molecular modeling and binding site prediction using the LeuTAa leucine transporter as a template. *Proteins: Struct., Funct., Bioinf.* **2008**, *70* (3), 1033–1046.

(34) Aronson, N. N.; Halloran, B. A.; Alexyev, M. F.; Amable, L.; Madura, J. D.; Pasupulati, L.; Worth, C.; Van Roey, P. Family 18 chitinase-oligosaccharide substrate interaction: Subsite preference and anomer selectivity of serratia marcescens chitinase A. *Biochem. J.* **2003**, *376* (Pt 1), 87–95.

(35) Oshiro, C.; Bradley, E. K.; Eksterowicz, J.; Evensen, E.; Lamb, M. L.; Lanctot, J. K.; Putta, S.; Stanton, R.; Grootenhuis, P. D. J. Performance Of 3D-Database Molecular Docking Studies into Homology Models. *J. Med. Chem.* **2004**, *47* (3), 764–767.

(36) Kairys, V.; Fernandes, M. X.; Gilson, M. K. Screening Drug-Like Compounds by Docking to Homology Models: A Systematic Study. *J. Chem. Inf. Model.* **2006**, *46* (1), 365–379.

(37) Martin, Y. C. 3D Database Searching In Drug Design. *J. Med. Chem.* **1992**, *35* (12), 2145–2154.

(38) Martin, Y. C.; Bures, M. G.; Danaher, E. A.; DeLazzer, J.; Lico, I.; Pavlik, P. A. A Fast New Approach To Pharmacophore Mapping And Its Application To Dopaminergic And Benzodiazepine Agonists. *J. Comput.-Aided Mol. Des.* **1993**, *7* (1), 83–102.

(39) Wang, S.; Zaharevitz, D. W.; Sharma, R.; Marquez, V. E.; Lewin, N. E.; Du, L.; Blumberg, P. M.; Milne, G. W. A. The Discovery of Novel, Structurally Diverse Protein Kinase C Agonists through Computer 3D-Database Pharmacophore Search. Molecular Modeling Studies. *J. Med. Chem.* **1994**, *37* (26), 4479–4489.

(40) Kaminski, J. J.; Rane, D. F.; Snow, M. E.; Weber, L.; Rothofsky, M. L.; Anderson, S. D.; Lin, S. L. Identification Of Novel Farnesyl Protein Transferase Inhibitors Using Three-Dimensional Database Searching Methods. *J. Med. Chem.* **1997**, *40* (25), 4103–4112.

(41) Nicklaus, M. C.; Neamati, N.; Hong, H.; Mazumder, A.; Sunder, S.; Chen, J.; Milne, G. W. A.; Pommier, Y. HIV-1 Integrase Pharmacophore: Discovery of inhibitors through three-dimensional database searching. *J. Med. Chem.* **1997**, *40* (6), 920–929.

(42) Wang, S.; Sakamuri, S.; Enyedy, I. J.; Kozikowski, A. P.; Deschaux, O.; Bandyopadhyay, B. C.; Tella, S. R.; Zaman, W. A.; Johnson, K. M. Discovery of a novel dopamine transporter inhibitor, 4-Hydroxy-1-methyl-4-(4-methylphenyl)-3-piperidyl 4-methylphenyl ketone, as a potential cocaine antagonist through 3D-database pharmacophore searching. Molecular modeling, structure-activity relationships, and behavioral pharmacological studies. *J. Med. Chem.* **2000**, *43* (3), 351–360.

(43) Indarte, M.; Liu, Y.; Madura, J. D.; Surratt, C. K. Receptor-Based Discovery of a Plasmalemmal Monoamine Transporter Inhibitor via High-Throughput Docking and Pharmacophore Modeling. *ACS Chem. Neurosci.* **2010**, *1* (3), 223–233.

(44) Shoichet, B. K. Virtual screening of chemical libraries. *Nature* **2004**, *432* (7019), 862–865.
(45) Nolan, T. L.; Lapinsky, D. J.; Talbot, J. N.; Indarte, M.; Liu, Y.; Manepalli, S.; Geffert, L. M.; Amos, M. E.; Taylor, P. N.; Madura, J. D.; Surratt, C. K. Identification of a novel selective serotonin reuptake inhibitor by coupling monoamine transporter-based virtual screening and rational molecular hybridization. *ACS Chem. Neurosci.* **2011**, d.o.i.10.1021/cn200044x.
(46) Shen, M.-Y.; Sali, A. Statistical potential for assessment and prediction of protein structures. *Protein Sci.* **2006**, *15* (11), 2507–2524.
(47) http://deposit.rcsb.org/validate (accessed Sep 30, 2010).
(48) Andersen, J.; Taboureau, O.; Hansen, K. B.; Olsen, L.; Egebjerg, J.; Stromgaard, K.; Kristensen, A. S. Location of the antidepressant binding site in the serotonin transporter: Importance of Ser-438 in recognition of citalopram and tricyclic antidepressants. *J. Biol. Chem.* **2009**, *284* (15), 10276–10284.
(49) Rupp, A.; Kovar, K. A.; Beuerle, G.; Ruf, C.; Folkers, G. A new pharmophoric model for 5-HT reuptake-inhibitors: Differentiation of amphetamine analogues. *Pharm. Acta Helv.* **1994**, *68* (4), 235–244.
(50) Muszynski, I. C.; Scapozza, L.; Kovar, K.-A.; Folkers, G. Quantitative Structure-Activity Relationships of Phenyltropanes as Inhibitors of Three Monoamine Transporters: Classical and CoMFA studies. *Quant. Struct.-Act. Relat.* **1999**, *18* (4), 342–253.
(51) Irwin, J. J.; Shoichet, B. K. ZINC--a free database of commercially available compounds for virtual screening. *J. Chem. Inf. Model.* **2005**, *45* (1), 177–182.
(52) Wang, W.; Sonders, M. S.; Ukairo, O. T.; Scott, H.; Kloetzel, M. K.; Surratt, C. K. Dissociation of High-Affinity Cocaine Analog Binding and Dopamine Uptake Inhibition at the Dopamine Transporter. *Mol. Pharmacol.* **2003**, *64* (2), 430–439.
(53) Ukairo, O. T.; Bondi, C. D.; Newman, A. H.; Kulkarni, S. S.; Kozikowski, A. P.; Pan, S.; Surratt, C. K. Recognition of Benztropine by the Dopamine Transporter (DAT) Differs from That of the Classical Dopamine Uptake Inhibitors Cocaine, Methylphenidate, and Mazindol as a Function of a DAT Transmembrane 1 Aspartic Acid Residue. *J. Pharmacol. Exp. Ther.* **2005**, *314* (2), 575–583.
(54) Anand, K.; Ziebuhr, J.; Wadhwani, P.; Mesters, J. R.; Hilgenfeld, R. Coronavirus Main Proteinase (3CLpro) Structure: Basis for Design of Anti-SARS Drugs. *Science* **2003**, *300* (5626), 1763–1767.
(55) Enyedy, I. J.; Lee, S.-L.; Kuo, A. H.; Dickson, R. B.; Lin, C.-Y.; Wang, S. Structure-Based Approach for the Discovery of Bis-benzamidines as Novel Inhibitors of Matriptase. *J. Med. Chem.* **2001**, *44* (9), 1349–1355.
(56) Enyedy, I. J.; Ling, Y.; Nacro, K.; Tomita, Y.; Wu, X.; Cao, Y.; Guo, R.; Li, B.; Zhu, X.; Huang, Y.; Long, Y.-Q.; Roller, P. P.; Yang, D.; Wang, S. Discovery of Small-Molecule Inhibitors of Bcl-2 through Structure-Based Computer Screening. *J. Med. Chem.* **2001**, *44* (25), 4313–4324.
(57) Li, R.; Chen, X.; Gong, B.; Selzer, P. M.; Li, Z.; Davidson, E.; Kurzban, G.; Miller, R. E.; Nuzum, E. O.; McKerrow, J. H.; Fletterick, R. J.; Gillmor, S. A.; Craik, C. S.; Kuntz, I. D.; Cohen, F. E.; Kenyon, G. L. Structure-based design of parasitic protease inhibitors. *Bioorg. Med. Chem.* **1996**, *4* (9), 1421–1427.
(58) Que, X.; Brinen, L. S.; Perkins, P.; Herdman, S.; Hirata, K.; Torian, B. E.; Rubin, H.; McKerrow, J. H.; Reed, S. L. Cysteine proteinases from distinct cellular compartments are recruited to phagocytic vesicles by Entamoeba histolytica. *Mol. Biochem. Parasitol.* **2002**, *119* (1), 23–32.
(59) Rajnarayanan, R. V.; Dakshanamurthy, S.; Pattabiraman, N. "Teaching old drugs to kill new bugs": Structure-based discovery of anti-SARS drugs. *Biochem. Biophys. Res. Commun.* **2004**, *321* (2), 370–378.
(60) Selzer, P. M.; Chen, X.; Chan, V. J.; Cheng, M.; Kenyon, G. L.; Kuntz, I. D.; Sakanari, J. A.; Cohen, F. E.; McKerrow, J. H. Leishmania major: Molecular Modeling of Cysteine Proteases and Prediction of New Nonpeptide Inhibitors. *Exp. Parasitol.* **1997**, *87* (3), 212–221.
(61) Zuccotto, F.; Zvelebil, M.; Brun, R.; Chowdhury, S. F.; Di Lucrezia, R.; Leal, I.; Maes, L.; Ruiz-Perez, L. M.; Gonzalez Pacanowska, D.; Gilbert, I. H. Novel inhibitors of Trypanosoma cruzi dihydrofolate reductase. *Eur. J. Med. Chem.* **2001**, *36* (5), 395–405.
(62) Consortium, T. U. The universal protein resource (UniProt). *Nucleic Acids Res.* **2007**, *35*, D193–D197.
(63) Berman, H. M.; Westbrook, J.; Feng, Z.; Gilliland, G.; Bhat, T. N.; Weissig, H.; Shindyalov, I. N.; Bourne, P. E. The Protein Data Bank. *Nucleic Acids Res.* **2000**, *28* (1), 235–242.
(64) *Discovery Studio Modeling Environment*, 2.5.1; Accelrys Software Inc.: San Diego, 2010.
(65) Sanchez, R.; Sali, A. Large-scale protein structure modeling of the Saccharomyces cerevisiae genome. *Proc. Natl. Acad. Sci. U. S. A.* **1998**, *95* (23), 13597–13602.
(66) Celik, L.; Sinning, S.; Severinsen, K.; Hansen, C. G.; Moller, M. S.; Bols, M.; Wiborg, O.; Schiott, B. Binding of Serotonin to the Human Serotonin Transporter. Molecular Modeling and Experimental Validation. *J. Am. Chem. Soc.* **2008**, *130* (12), 3853–3865.
(67) Beuming, T.; Shi, L.; Javitch, J. A.; Weinstein, H. A Comprehensive Structure-Based Alignment of Prokaryotic and Eukaryotic Neurotransmitter/Na Symporters (NSS) Aids in the Use of the LeuT Structure to Probe NSS Structure and Function. *Mol. Pharmacol.* **2006**, *70* (5), 1630–1642.
(68) Molecular Operating Environment (MOE); Chemical Computing Group Inc., S. S. W., Suite #910, Montreal, QC, Canada, H3A 2R7.
(69) Ponder, J. W.; Case, D. A. Force fields for protein simulations. *Adv. Protein Chem.* **2003**, *66*, 27–85.
(70) Wang, J.; Cieplak, P.; Kollman, P. A. How well does a restrained electrostatic potential (RESP) model perform in calculating conformational energies of organic and biological molecules? *J Comput. Chem.* **2000**, *21* (12), 1049–1074.
(71) The Cambridge Structural Database: a quarter of a million crystal structures and rising, Frank, H. The Cambridge Structural Database: a quarter of a million crystal structures and rising. *Acta Crystallogr., Sect. B: Struct. Sci.* **2002**, *B58* (3, No. 1), 380–388.
(72) McMeeking, B.; Fletcher, D. The United Kingdom Chemical Database Service: CDS. *Cheminf. Dev.* **2004**, 37–67.
(73) Halgren, T. A. Merck molecular force field. I. Basis, form, scope, parameterization, and performance of MMFF94. *J. Comput. Chem.* **1996**, *17* (5 & 6), 490–519.
(74) Halgren, T. A. Force fields: MMFF94. In *Encyclopedia of computational chemistry*; 1998; Vol. 2, pp 1033−1035.
(75) Maple, Forcefields: A general discussion. *Encyclopedia of computational chemistry*; 1998; Vol 2, pp 1015−1024.
(76) Clark, A. M.; Labute, P. 2D depiction of protein-ligand complexes. *J. Chem. Inf. Model.* **2007**, *47* (5), 1933–1944.
(77) Lipinski, C. A.; Lombardo, F.; Dominy, B. W.; Feeney, P. J. Experimental and computational approaches to estimate solubility and permeability in drug discovery and development settings. *Adv. Drug Delivery Rev.* **2001**, *46* (1−3), 3–26.
(78) Cheng, Y.; Prusoff, W. H. Relationship between the inhibition constant (KI) and the concentration of inhibitor which causes 50% inhibition (I50) of an enzymatic reaction. *Biochem. Pharmacol.* **1973**, *22* (23), 3099–3108.
(79) Beitz, E. TEXshade: Shading and labeling of multiple sequence alignments using LATEX2 epsilon. *Bioinformatics* **2000**, *16* (2), 135–139.